

# **A high speed PE-ALD ZnO Schottky diode rectifier with low interface-state density**

Jidong Jin<sup>1,5</sup>, Jiawei Zhang<sup>2</sup>, Andrew Shaw<sup>1</sup>, Valeriya N. Kudina<sup>3</sup>, Ivona Z. Mitrovic<sup>1</sup>, Jacqueline S. Wrench<sup>4</sup>, Paul R. Chalker<sup>4</sup>, Claudio Balocco<sup>5</sup>, Aimin Song<sup>2</sup> and Steve Hall<sup>1</sup>

<sup>1</sup>Department of Electrical Engineering and Electronics, University of Liverpool, Liverpool, L69 3GJ, United Kingdom.

<sup>2</sup>School of Electrical and Electronic Engineering, University of Manchester, Manchester, M13 9PL, United Kingdom.

<sup>3</sup>Lashkaryov Institute of Semiconductor Physics, National Academy of Sciences of Ukraine, Prospekt Nauki 41, Kyiv 03028, Ukraine

<sup>4</sup>Centre for Materials and Structures, School of Engineering, University of Liverpool, Liverpool L69 3GH, United Kingdom

<sup>5</sup>Department of Engineering, Durham University, Durham DH1 3LE, United Kingdom

Authors to whom correspondence should be addressed. E-mail: S.Hall@liverpool.ac.uk

## **Abstract**

Zinc oxide (ZnO) has recently attracted attention for its potential application to high speed electronics. In this work, a high speed Schottky diode rectifier was fabricated based on a ZnO thin film deposited by plasma-enhanced atomic layer deposition and a PtO<sub>x</sub> Schottky contact deposited by reactive radio-frequency sputtering. The rectifier shows an ideality factor of 1.31, an effective barrier height of 0.79 eV, a rectification ratio of  $1.17 \times 10^7$ , and cut-off frequency as high as 550 MHz. Low frequency noise measurements reveal that the rectifier has a low interface-state density of  $5.13 \times 10^{12} \text{ cm}^{-2} \text{ eV}^{-1}$ , and the noise is dominated by mechanism of random walk of electrons at the PtO<sub>x</sub>/ZnO interface. The work shows that the rectifier can be used for both noise sensitive and high frequency electronics applications.

Keywords: zinc oxide, plasma-enhanced atomic layer deposition, Schottky diode, rectifier

## 1. Introduction

Oxide semiconductors exhibit a wide range of interesting optical and electronic properties and have drawn significant interest from the electronics industry [1, 2]. Schottky diodes based on oxide semiconductor materials such as zinc oxide (ZnO) and indium gallium zinc oxide (IGZO) have rapidly gained popularity as high speed rectifiers in recent years [3-7]. The cut-off frequency of a Schottky diode rectifier is inversely proportional to the product of the series resistance ( $R_s$ ) and junction capacitance ( $C_D$ ) [4, 7]. Two common approaches for improving the cut-off frequency are the use of semiconductor materials with high mobility to minimize series resistance [7] and the use of smaller device layout to reduce the junction capacitance [3, 4]. By optimizing  $R_s$  and  $C_D$ , oxide based rectifiers are capable of operating well into the ultra-high frequency (UHF) band [3, 4]. Moreover, the use of a semiconductor material with low carrier concentration is essential to avoid tunneling of charge carriers at the Schottky contact. At low carrier concentration,  $qE_{oo} / kT \leq 1$  and thermionic emission is the dominant current-transport mechanism [8], where  $q$  is the electron charge,  $E_{oo}$  is the tunneling parameter,  $k$  is Boltzmann's constant, and  $T$  is the absolute temperature. The incorporation of metal cations such as Ga and In into ZnO to form so-called IGZO serves to control the carrier concentration [9, 10]. In turn, this incorporation can enhance the electrical properties of Schottky diodes fabricated in these materials [5]. As an alternative approach, Jin *et al.* recently developed an effective deposition methodology to control ZnO carrier concentration without extrinsic doping by the use of plasma-enhanced atomic layer deposition (PE-ALD) [11]. It was found that controlling the ZnO carrier concentration required the PE-ALD process to be conducted at a low temperature and with a relatively long oxygen plasma time. However, the low temperature PE-ALD process results in low mobility of ZnO films [12]. One possible way to overcome this problem is post-thermal annealing, which serves to improve the crystallinity and mobility of the ZnO film [13]. Defect states at the metal-semiconductor interface influence the Schottky barrier height and hence influence the performance of the diodes [14, 15]. Oxidized metal Schottky contacts, such as silver oxide ( $Ag_xO$ ) and platinum oxide ( $PtO_x$ ), have been widely used to reduce the interface defect states

between ZnO and Schottky contacts to achieve good rectification properties [16]. The ZnO Schottky contacts which use Ag<sub>x</sub>O films can result in ideality factors very close to unity [15], but they can decompose at 200 °C in air [17]. In contrast, PtO<sub>x</sub> films are thermally stable up to 500 °C in air [18]. In the last few decades, the low-frequency noise (LFN) properties of Schottky diodes have been widely investigated [19-23]. To date, LFN properties of Schottky diodes based on ZnO nanorods have been reported [24]. However, characterization of the LFN of ultra-fast Schottky diodes based on PE-ALD ZnO thin films has remained unexplored.

Here, we report the use of ZnO Schottky diode as a high speed rectifier. The diode is based on a ZnO thin film deposited by PE-ALD, and a PtO<sub>x</sub> Schottky contact deposited by reactive radio-frequency sputtering. Prior to measurements, the diode was annealed at 300 °C in air for 1 hour to improve the mobility and crystallinity of the ZnO film (see Supplementary Information). Firstly, the current-voltage (*I-V*) and capacitance-voltage (*C-V*) characteristics of the diode were measured and analyzed. Secondly, high frequency measurements were carried out. Finally, the LFN properties of the diode were investigated.

## 2. Experiments

### 2.1. Device Fabrication

The diodes were fabricated on Corning 7059 glass substrate. Standard photolithography was used to pattern the metal contacts. A Moorfield nanoPVD sputter system was used for the metal deposition. Figure 1a shows the schematic of the Schottky diode used in this study. A 70 nm thick Ti electrode was deposited on the glass substrate by radio frequency (RF) sputtering at 73 W, with pure Ar at a chamber pressure of  $3.5 \times 10^{-3}$  mbar. The samples were then loaded into an Oxford Instruments Plasma OPAL reactor to deposit 90 nm PE-ALD ZnO thin film. ZnO film was deposited at 80 °C with an O<sub>2</sub> plasma time of 50 s [11]. ZnO mesa isolation was then performed using photolithography and acetic acid etching solution to define the active device area. The etch rate of ZnO strongly depends on the acetic acid concentration. If the acetic acid concentration is too high, there is poor etch controllability and

reproducibility. On the other hand, low concentrations result in rough edges. We have conducted etch studies and found that 1% acetic acid etching solution gives an optimal etch rate of 2.5 nm/s. The total etch time was 36s. After the active area was defined, 60 nm  $\text{PtO}_x$  was deposited by reactive RF sputtering in  $\text{Ar}/\text{O}_2$  with a flow rate of 1 / 1 sccm using the Pt target (99.95%) and RF power of 73 W. Subsequently, an additional 10 nm Pt capping layer was deposited on  $\text{PtO}_x$  by RF sputtering. The overlapping region between Ti ohmic contact and  $\text{PtO}_x$  Schottky contact determines the effective area of the diode, which is  $600 \mu\text{m}^2$ . Finally, the devices were annealed at  $300 \text{ }^\circ\text{C}$  in air for 1 hour to improve the mobility of the ZnO.

## 2.2 Device Characterization

The  $I$ - $V$  and  $C$ - $V$  characteristics were measured using a semiconductor parameter analyzer (Agilent B1500) and an impedance analyzer (Agilent E4980A) at 10 kHz, respectively. A coplanar probe was used to deliver an RF signal, generated by a network analyser (Agilent E5061B), to the ZnO Schottky diodes for high frequency characterization. The output voltage was measured using an Agilent 34401A multimeter. The LFN was measured using a SR570 low noise current amplifier and a NI USB-6211 data acquisition module at different biases in an isolated metal box which provides electromagnetic screening.

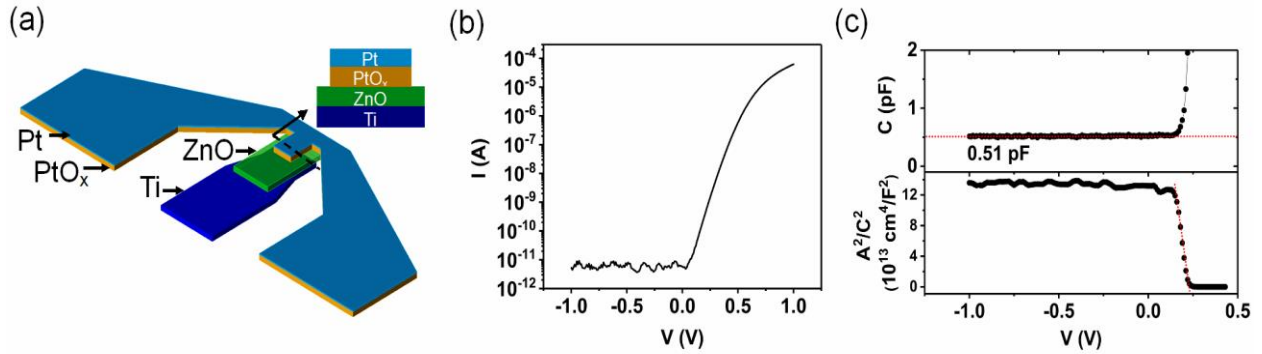


**Figure 1.** a) Schematic diagram of the ZnO Schottky diode. b)  $I$ - $V$  characteristic of the ZnO Schottky diode. c)  $C$ - $V$  and  $A^2/C^2$ - $V$  characteristic of the ZnO Schottky diode.  $V_{bi}$  and  $N_{dep}$  values are extracted from the gradient of the dashed line from the  $A^2/C^2$ - $V$  plot.

### 3. Results and discussion

Figure 1b shows a typical  $I$ - $V$  characteristic of a ZnO Schottky diode. An excellent rectifying characteristic was obtained, with a rectification ratio of  $1.17 \times 10^7$  at  $\pm 1$  V. The current transport through a Schottky diode can be described by the thermionic emission model

$$I = I_s \left\{ \exp \left[ \frac{q(V - IR_s)}{nkT} \right] - 1 \right\} \quad (1)$$

$$I_s = AA^*T^2 \exp \left( -\frac{q\phi_B}{kT} \right) \quad (2)$$

where  $I_s$  is the saturation current,  $A$  is the effective area of the diode,  $A^*$  is the effective Richardson constant with a theoretical value of  $32 \text{ A cm}^{-2} \text{ K}^{-2}$  for ZnO [25],  $\phi_B$  is the effective barrier height, and  $n$  is the ideality factor. Fitting the forward  $I$ - $V$  curve with Equations 1 and 2 yields,  $n=1.31$  and  $\phi_B = 0.79$  eV. It should be noted that the relatively large value of  $n=1.31$  can be explained by the contribution of PtO<sub>x</sub>/ZnO interface states and contact inhomogeneity which gives rise to a statistical variation of barrier heights across the diode [15, 25, 26] as a result of the nano-crystalline nature of the material (see Supplementary Information). The diode series resistance,  $R_s$  was determined from a plot of  $dV/dI$  vs  $V$  to give a value  $4.5 \text{ k}\Omega$  [27] (see figure S3, Supplementary Information).

The  $C$ - $V$  characteristic of the diode measured at 10 kHz is shown in figure 1c. At negative bias, the capacitance remains almost constant, suggesting that the ZnO film is fully depleted. The small effective area of the diode limits the depletion layer capacitance to 0.51 pF, which enables a high speed operation. The built-in potential,  $V_{bi}$ , and the net doping density,  $N_{dep}$ , can be determined from a plot of  $A^2/C^2$  vs  $V$ , using

$$\frac{A^2}{C^2} = \left( \frac{2}{\epsilon_o \epsilon_s N_{dep}} \right) \left( V_{bi} - \frac{kT}{q} - V \right), \quad (3)$$

where  $\epsilon_0$  is the permittivity of free space, and  $\epsilon_s$  is the dielectric constant of the semiconductor (8.5 for ZnO) [11]. From the  $A^2/C^2$  vs  $V$  plot shown in figure 1c,  $N_{dep}$  is determined to be  $8.32 \times 10^{15} \text{ cm}^{-3}$  and  $V_{bi}$  is found to be 0.24 V.

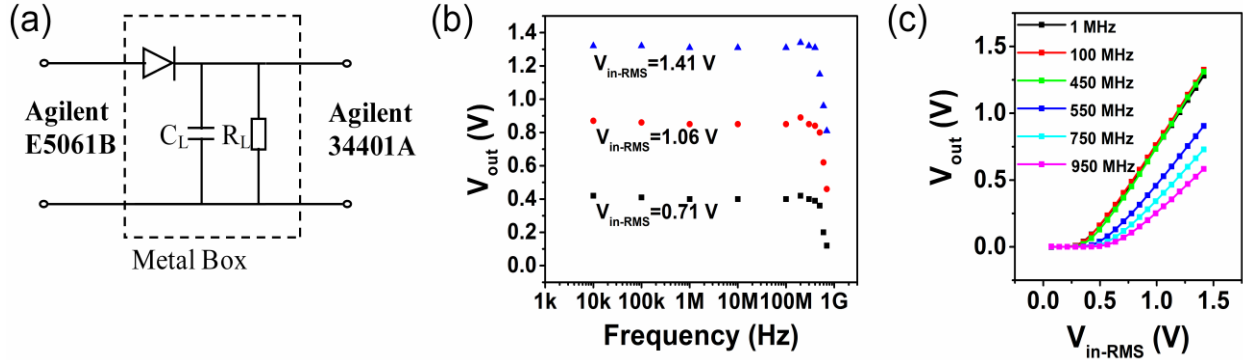


**Figure 2.** a) Schematic diagram of the high-frequency measurement circuit. b) Output DC voltages as a function of the input frequency at different input RF signal strengths. c) Output DC voltages as a function of the input RF signal voltages at different frequencies.

The high-frequency measurement system is shown in figure 2a. The signal was generated by an Agilent E5061B network analyzer and the output voltage across the load resistor,  $R_L = 10 \text{ M}\Omega$ , and load capacitor,  $C_L = 0.1 \text{ }\mu\text{F}$ , was measured using an Agilent 34401A multimeter. Figure 2b shows the DC output voltage versus frequency at different input RF signal strength. Input RF signals are expressed with root-mean-square voltage ( $V_{in-RMS}$ ). For frequency values between 10 kHz and 100 MHz, the output remained nearly constant at each input voltage. The slight rise in output peak observed at 200 MHz is most likely due to impedance mismatch in the measurement system [28]. Figure 2c shows DC output voltage versus the input RF signal voltage at different frequencies. When the input signal frequency was higher than 500 MHz, the output voltage starts to drop. It is seen that the diode rectifier can be operated with a cut-off frequency (also known as -3 dB frequency) as high as 550 MHz, which covers the very high frequency band (30 MHz to 300 MHz) and part of the UHF band (300 MHz to 3 GHz). This operating frequency

enables the PE-ALD ZnO Schottky diode to be considered as a promising high speed device for future wireless transmission systems.

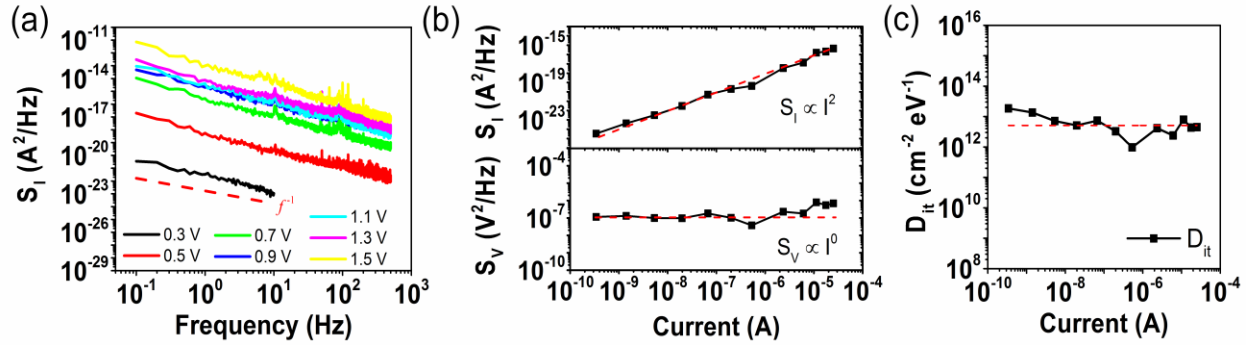


**Figure 3.** a) Current noise spectra of the ZnO Schottky diode at different biases. b) Current and voltage noises as a function of current at 5 Hz. c) Interface trap density as a function of current.

Low frequency noise is an important factor which limits the practical detection sensitivity and resolution of Schottky diodes when used in microwave applications [29, 30]. Figure 3a shows the plot of current noise ( $S_I$ ) as a function of frequency ( $f$ ) measured under different bias conditions. At low frequencies, the spectra are dominated by flicker noise, where  $S_I \propto f^{-1}$ . In general, the  $1/f$  component in the noise spectra of Schottky diodes can come from a range of different noise sources, namely, fluctuations in the occupancy of bulk traps [19], mobility and diffusivity fluctuation [31], random walk electrons at interfaces [21], and series resistance [32]. An analysis of the dependencies of  $S_I$  on  $I$  and total voltage noise ( $S_V$ ) on  $I$  can be used to ascertain which noise model describes the  $1/f$  noise behavior of the ZnO diode. These dependencies measured at  $f = 5$  Hz are shown in figure 3b. In figure 3b,  $S_I \propto I^2$  allows us to exclude the mobility and diffusivity fluctuation model from consideration, since it exhibits  $S_I \propto I$  [23, 31].  $S_V$  can be expressed as

$$S_V = S_{I,dep} \left( \frac{dV}{dI} \right)^2 + S_{I,series} R_s^2 \quad (4)$$

where  $S_{I,dep}$  is the current noise originating in bulk traps or interface states,  $S_{I,series}=I^2\alpha_H/fN_{total}$  is the current noise originating in the series resistance, and  $N_{total}$  is the total number of free carriers and  $\alpha_H$  is Hooge's constant [32]. According to Equation (4), if the  $1/f$  noise is dominated by the series resistance contribution, then the value of  $S_V$  should be proportional to  $I^2$ . However, as shown in figure 3b, the voltage noise is almost independent of  $I$ , which indicates that the  $1/f$  noise of the ZnO Schottky diode is not affected by the series resistance. For the  $1/f$  noise arising from bulk traps or interface states,  $(dV/dI)^2$  is proportional to  $I^2$ , and  $S_V$  should remain the same at different currents.

The  $1/f$  noise from bulk traps can be described by Hsu's trapping model [19]. However, this model does not take into account the role of interface states, which cannot be assumed as negligible for our diode. As mentioned earlier, the relatively large value of  $n=1.31$  can be explained by the contribution of PtO<sub>x</sub>/ZnO interface states and contact inhomogeneity. In this respect, it should be expected that the  $1/f$  noise mainly originates in the PtO<sub>x</sub>/ZnO interface states which are described in the random walk model. In the random walk model, the noise is related to the interface-state density [21, 33],  $D_{it}$ , which is described as:

$$S_{I,dep} = \frac{0.1}{f} \left( \frac{qI}{4\epsilon_o\epsilon_s} \right)^2 \frac{q^2 D_{it}}{kT\pi N_{dep} WA} \quad (5)$$

where  $W$  is the depletion width, and  $A$  is the active area of the diode. According to Equation (5), the interface-state density is calculated to be  $5.13 \times 10^{12} \text{ cm}^{-2} \text{ eV}^{-1}$  (see figure 3c). This is around one order of magnitude smaller than the values for Ag/single crystalline ZnO ( $6.83 \times 10^{13} \text{ cm}^{-2} \text{ eV}^{-1}$ ) [34], and Au/ZnO ( $4.2 \times 10^{13} \text{ cm}^{-2} \text{ eV}^{-1}$ ) [35]. The low interface-state density found for the ZnO Schottky diode makes it suitable for noise-sensitive applications such as frequency mixers, photo-sensors, and microwave detectors.

## Conclusions

In conclusion, we have fabricated a high speed rectifier based on a ZnO film deposited by PE-ALD without the need for doping and a PtO<sub>x</sub> Schottky contact deposited by reactive radio-frequency sputtering. The rectifier shows an ideality factor of 1.31, an effective barrier height of 0.79 eV, a rectification ratio of



$1.17 \times 10^7$ , and cut-off frequency as high as 550 MHz. The LFN measurements reveal that the rectifier has a low interface-state density of  $5.13 \times 10^{12} \text{ cm}^{-2} \text{ eV}^{-1}$ , and that the noise is dominated by the mechanism of the random walk of electrons at the  $\text{PtO}_x/\text{ZnO}$  interface. The results demonstrate that the use of PE-ALD ZnO films and  $\text{PtO}_x$  Schottky contacts can provide a viable pathway for delivering high performance rectifiers for both noise sensitive and high frequency electronic applications.

### Acknowledgements

This research has been funded by the United Kingdom Engineering and Physical Research Council (EPSRC) Grant EP/K018884/1 and EP/N021258/1. A.S. acknowledges EPSRC for funding his PhD studies.

### References

- [1] Kim Y-H, Heo J-S, Kim T-H, Park S, Yoon M-H, Kim J, Oh M S, Yi G-R, Noh Y-Y and Park S K 2012 Flexible metal-oxide devices made by room-temperature photochemical activation of sol-gel films. *Nature* **489** 128
- [2] Yu X, Marks T J and Facchetti A 2016 Metal oxides for optoelectronic applications. *Nat. Mater.* **15** 383
- [3] Chasin A, Nag M, Bhoelokam A, Myny K, Steudel S, Schols S, Genoe J, Gielen G and Heremans P 2013 Gigahertz Operation of a-IGZO Schottky Diodes. *IEEE Trans. Electron Devices* **60** 3407
- [4] Chasin A, Volskiy V, Libois M, Myny K, Nag M, Rockele M, Vandenbosch G A E, Genoe J, Gielen G and Heremans P 2014 An Integrated a-IGZO UHF Energy Harvester for Passive RFID Tags. *IEEE Trans. Electron Devices* **61** 3289
- [5] Zhang J, Li Y, Zhang B, Wang H, Xin Q and Song A 2015 Flexible indium–gallium–zinc–oxide Schottky diode operating beyond 2.45 GHz. *Nat. Commun.* **6** 7561
- [6] Zhang J, Wang H, Wilson J, Ma X, Jin J and Song A 2016 Room Temperature Processed Ultrahigh-Frequency Indium-Gallium-Zinc-Oxide Schottky Diode. *IEEE Electron Device Lett.* **37** 389
- [7] Semple J, Rossbauer S, Burgess C H, Zhao K, Jagadamma L K, Amassian A, McLachlan M A and Anthopoulos T D 2016 Radio Frequency Coplanar ZnO Schottky Nanodiodes Processed from Solution on Plastic Substrates. *Small* **12** 1993
- [8] Rhoderick E H and Williams R H 1988 *Metal-Semiconductor Contacts*. Oxford, Clarendon Press

- [9] Nomura K, Takagi A, Kamiya T, Ohta H, Hirano M and Hosono H 2006 Amorphous Oxide Semiconductors for High-Performance Flexible Thin-Film Transistors. *Jpn. J. Appl. Phys.* **45** 4303
- [10] Olziersky A, Barquinha P, Vilà A, Magaña C, Fortunato E, Morante J R and Martins R 2011 Role of  $\text{Ga}_2\text{O}_3$ - $\text{In}_2\text{O}_3$ -ZnO channel composition on the electrical performance of thin-film transistors. *Mater. Chem. Phys.* **131** 512
- [11] Jin J, Wrench J S, Gibbon J T, Hesp D, Shaw A, Mitrovic I Z, Sedghi N, Phillips L J, Zou J, Dhanak V R, Chalker P R and Hall S 2017 Schottky Diodes on ZnO Thin Films Grown by Plasma-Enhanced Atomic Layer Deposition. *IEEE Trans. Electron Devices* **64** 1225
- [12] Kim D, Kang H, Kim J-M and Kim H 2011 The properties of plasma-enhanced atomic layer deposition (ALD) ZnO thin films and comparison with thermal ALD. *Appl. Surf. Sci.* **257** 3776
- [13] Fortunato E M C, Barquinha P M C, Pimentel A C M B G, Gonçalves A M F, Marques A J S, Pereira L M N and Martins R F P 2005 Fully Transparent ZnO Thin-Film Transistor Produced at Room Temperature. *Adv. Mater.* **17** 590
- [14] Ip K, Thaler G T, Yang H, Han S Y, Li Y, Norton D P, Pearton S J, Jang S and Ren F 2006 Contacts to ZnO. *J. Cryst. Growth* **287** 149
- [15] Brillson L J and Lu Y 2011 ZnO Schottky barriers and Ohmic contacts. *J. Appl. Phys.* **109** 121301
- [16] Allen M W, Mendelsberg R J, Reeves R J, and Durbin S M 2009 Oxidized noble metal Schottky contacts to n-type ZnO. *Appl. Phys. Lett.* **94** 103508
- [17] Pierson J F and Rousselot C 2005 Stability of reactively sputtered silver oxide films. *Surf. Coat. Technol.* **200** 276
- [18] Abe Y, Kawamura M and Sasaki K 1999 Preparation of PtO and  $\alpha$ -PtO<sub>2</sub> Thin Films by Reactive Sputtering and Their Electrical Properties. *Jpn. J. Appl. Phys.* **38** 2092
- [19] Hsu S T 1971 Flicker noise in metal semiconductor Schottky barrier diodes due to multistep tunneling processes. *IEEE Trans. Electron Devices* **18** 882
- [20] Luo M Y, Bosman G, Ziel A V D and Hench L L 1988 Theory and experiments of 1/f noise in Schottky-barrier diodes operating in the thermionic-emission mode. *IEEE Trans. Electron Devices* **35** 1351
- [21] Lee J I, Brini J, Chovet A and Dimitriadis C A 1999 Flicker noise by random walk of electrons at the interface in nonideal Schottky diodes. *Solid-State Electron.* **43** 2185
- [22] Papatzika S, Hastas N A, Angelis C T, Dimitriadis C A, Kamarinos G and Lee J I 2002 Investigation of noise sources in platinum silicide Schottky barrier diodes. *Appl. Phys. Lett.* **80** 1468
- [23] Zhang J, Zhang L, Ma X, Wilson J, Jin J, Du L, Xin Q and Song A 2015 Low-frequency noise properties in Pt-indium gallium zinc oxide Schottky diodes. *Appl. Phys. Lett.* **107** 093505
- [24] Chen T P, Young S J, Chang S J, Hsiao C H, Ji L W, Hsu Y J and Wu S L 2013 Low-Frequency Noise Characteristics of ZnO Nanorods Schottky Barrier Photodetectors. *IEEE Sens. J.* **13** 2115
- [25] Müller S, Wenckstern H v, Schmidt F, Splith D, Heinhold R, Allen M and Grundmann M 2014 Method of choice for fabrication of high-quality ZnO-based Schottky diodes. *J. Appl. Phys.* **116** 194506
- [26] Tung R T 2001 Recent advances in Schottky barrier concepts. *Mater. Sci. Eng. R.* **35** 1

- [27] Gökçen M, Altındal Ş, Karaman M and Aydemir U 2011 Forward and reverse bias current–voltage characteristics of Au/n-Si Schottky barrier diodes with and without SnO<sub>2</sub> insulator layer. *Physica B* **406** 4119
- [28] Sani N, Robertsson M, Cooper P, Wang X, Svensson M, Ersman P A, Norberg P, Nilsson M, Nilsson D, Liu X, Hesselbom H, Akesso L, Fahlman M, Crispin X, Engquist I, Berggren M and Gustafsson G 2014 All-printed diode operating at 1.6 GHz. *Proc. Natl Acad. Sci.* **111** 11943
- [29] Rizzoli V, Mastri F and Masotti D 1994 General noise analysis of nonlinear microwave circuits by the piecewise harmonic-balance technique. *IEEE Trans. Microwave Theory Tech.* **42** 807
- [30] Young A C, Zimmerman J D, Brown E R and Gossard A C 2007 Low-frequency noise in epitaxially grown Schottky junctions. *J. Appl. Phys.* **101** 084509
- [31] Kleinpenning T G M 1979 Low-frequency noise in Schottky barrier diodes. *Solid-State Electron.* **22** 121
- [32] Hooge F N 1969  $1/f$  noise is no surface effect. *Phys. Lett. A* **29** 139
- [33] Jantsch O 1987 Flicker ( $1/f$ ) noise generated by a random walk of electrons in interfaces. *IEEE Trans. Electron Devices* **34** 1100
- [34] Kim H, Kim H and Kim D-W 2014 Effect of oxygen plasma treatment on the electrical properties in Ag/bulk ZnO Schottky diodes. *Vacuum* **101** 92
- [35] Aydoğan Ş, Çınar K, Asıl H, Coşkun C and Türüt A 2009 Electrical characterization of Au/n-ZnO Schottky contacts on n-Si. *J. Alloys Compd.* **476** 913

# Supplementary Information

## A high speed PE-ALD ZnO Schottky diode rectifier with low interface-state density

Jidong Jin<sup>1,5</sup>, Jiawei Zhang<sup>2</sup>, Andrew Shaw<sup>1</sup>, Valeriya N. Kudina<sup>3</sup>, Ivona Z. Mitrovic<sup>1</sup>, Jacqueline S. Wrench<sup>4</sup>, Paul R. Chalker<sup>4</sup>, Claudio Balocco<sup>5</sup>, Aimin Song<sup>2</sup> and Steve Hall<sup>1</sup>

<sup>1</sup>Department of Electrical Engineering and Electronics, University of Liverpool, Liverpool, L69 3GJ, United Kingdom.

<sup>2</sup>School of Electrical and Electronic Engineering, University of Manchester, Manchester, M13 9PL, United Kingdom.

<sup>3</sup>Lashkaryov Institute of Semiconductor Physics, National Academy of Sciences of Ukraine, Prospekt Nauki 41, Kyiv 03028, Ukraine

<sup>4</sup>Centre for Materials and Structures, School of Engineering, University of Liverpool, Liverpool L69 3GH, United Kingdom

<sup>5</sup>Department of Engineering, Durham University, Durham DH1 3LE, United Kingdom

### 1. Mobility extraction

Bottom-gate thin film transistors (TFTs) were fabricated to allow extraction of effective field carrier mobility of the ZnO film. Highly doped *n*-type silicon with a 50 nm thermally oxidized SiO<sub>2</sub> layer was used as the substrate. The highly doped *n*-type silicon acts as the gate electrode. ZnO films were deposited on SiO<sub>2</sub> by PE-ALD at 80 °C with an O<sub>2</sub> plasma time of 50 s. Al source/drain contacts with a thickness of 80 nm were deposited on ZnO film by thermal evaporation through a shadow mask, defining a TFT channel width  $W=2000\ \mu\text{m}$  and a channel length  $L=60\ \mu\text{m}$ . Initially, the transfer and output characteristics of the TFT were measured. Then, the device was annealed in air at 300 °C for 1 hour. Finally, the transfer and output characteristics of the TFT were measured again for the annealed device.

The effective saturation mobility ( $\mu_{sat}$ ) was obtained using the standard equation for source-drain saturation current

$$I_{DS} = \frac{W}{2L} C_i \mu_{sat} (V_{GS} - V_T)^2 \text{ for } V_{DS} > V_{GS} - V_T \quad (S1)$$

where  $C_i$  is the gate capacitance per unit area,  $V_T$  is the threshold voltage,  $V_{GS}$  is the gate voltage, and  $V_{DS}$  is the drain voltage.

It should be noted that the post-thermal annealing significantly improved the field effect mobility of ZnO. After annealing,  $\mu_{sat}$  was improved from  $7.70 \times 10^{-4} \text{ cm}^2/\text{Vs}$  to  $0.34 \text{ cm}^2/\text{Vs}$ .

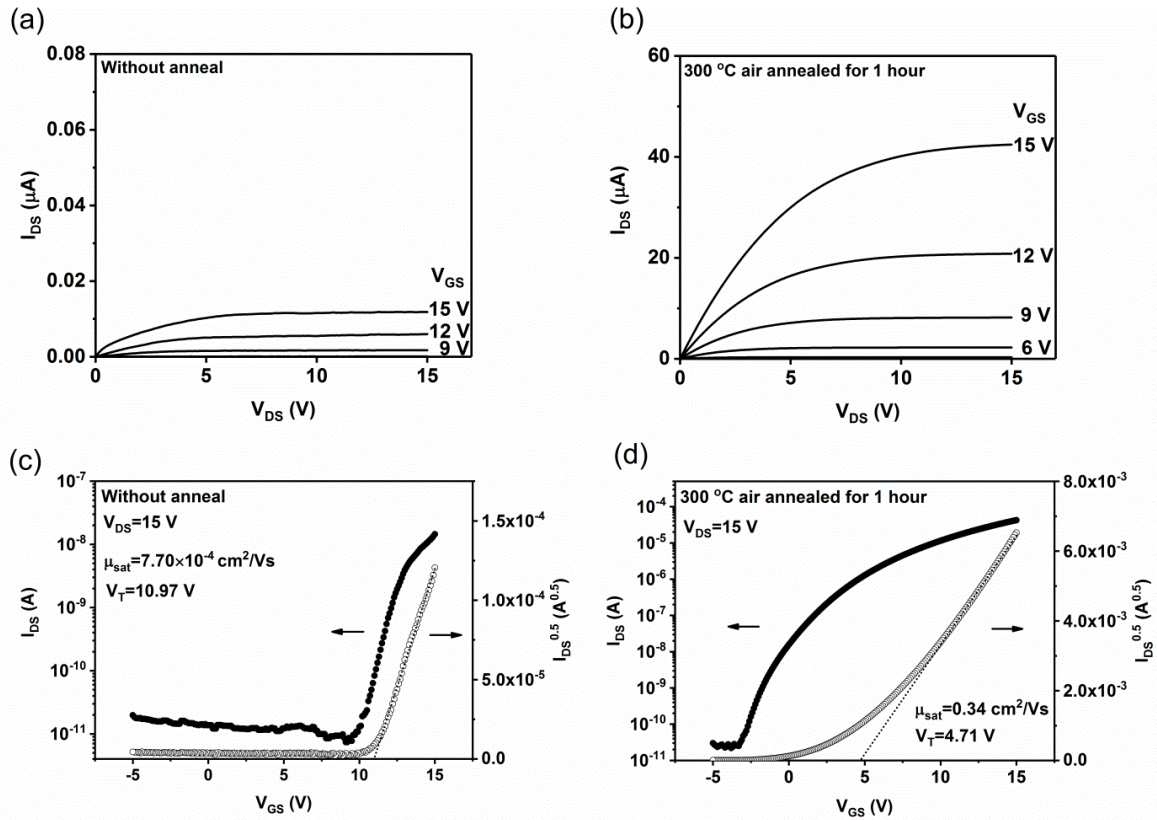


Figure S1. Output characteristics of the ZnO TFTs measured (a) without annealing and (b) after annealing at 300 °C in air for 1 hour. Transfer characteristics of the ZnO TFTs measured (c) without annealing and (d) after annealing at 300 °C in air for 1 hour.

## 2. X-ray diffraction investigation

ZnO film was deposited on glass by PE-ALD at 80 °C with an O<sub>2</sub> plasma time of 50 s. The crystal structures of this ZnO film were characterized by X-ray diffraction (XRD). Then, the sample was annealed in air at 300 °C for 1 hour and investigated by XRD to determine the crystal structure. For both as-deposited and annealed films, (100) and (002) peaks were observed. The act of annealing in air enhances the film crystallinity, as indicated by the reduction of full width at half maxima (FWHM) of both the (100) and (002) peak, from 0.401 to 0.381 and 0.346 to 0.299, respectively. Grain size was estimated using the Scherrer formula applied to the (100) and (002) reflections. After annealing in air, the grain size increased from approximately 25.6 to 28.4 nm, indicating that the grain boundary network cross section becomes effectively smaller, reducing the carrier scattering. This reduction leads to the increase in electron mobility.

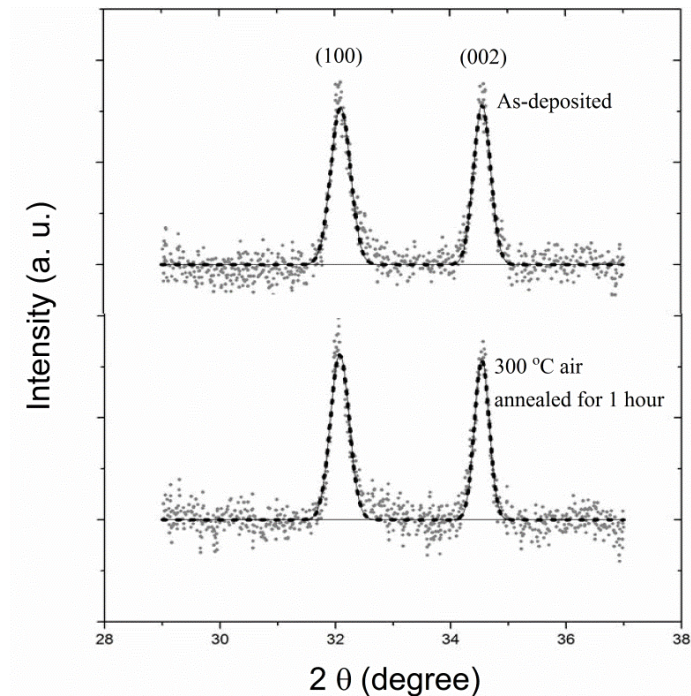


Figure S2. X-ray diffraction of PE-ALD ZnO film as-deposited and annealed in air at 300 °C for 1 hour.

### 3. Series resistance determination

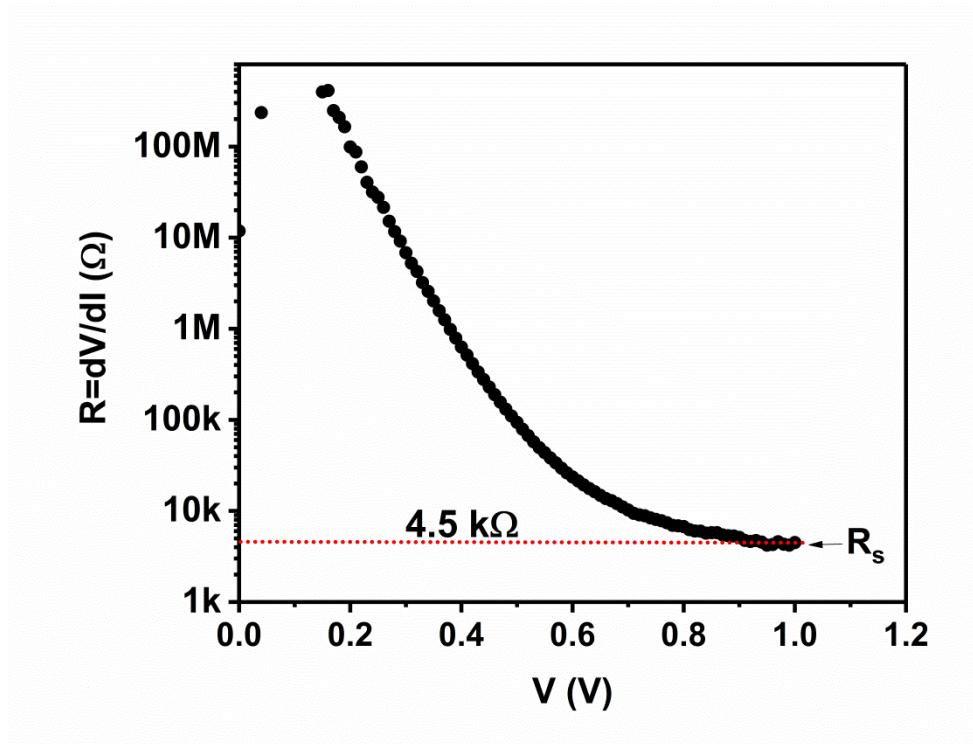


Figure S3. Resistance of the ZnO Schottky diode as a function of forward voltage.